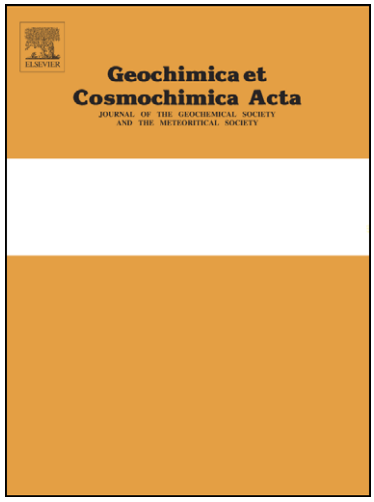

Competition effects in cation binding to Humic Acid. Conditional affinity spectra for fixed total metal concentration conditions

Calin David, Sandrine Mongin, Carlos Rey-Castro, Josep Galceran, Encarnació Companys, José Luis Garcés, José Salvador, Jaume Puy, Joan Cecilia, Pablo Lodeiro, Francesc Mas

PII: S0016-7037(10)00364-9
DOI: 10.1016/j.gca.2010.06.023
Reference: GCA 6821

To appear in: *Geochimica et Cosmochimica Acta*

Received Date: 19 February 2010
Accepted Date: 18 June 2010

Please cite this article as: David, C., Mongin, S., Rey-Castro, C., Galceran, J., Companys, E., Garcés, J.L., Salvador, J., Puy, J., Cecilia, J., Lodeiro, P., Mas, F., Competition effects in cation binding to Humic Acid. Conditional affinity spectra for fixed total metal concentration conditions, *Geochimica et Cosmochimica Acta* (2010), doi: 10.1016/j.gca.2010.06.023

Competition effects in cation binding to Humic Acid. Conditional affinity spectra for fixed total metal concentration conditions

Calin David[a)], Sandrine Mongin[a)], Carlos Rey-Castro[a)], Josep Galceran[a)], Encarnació Companys[a)], José Luis Garcés[a)], José Salvador[a)], Jaume Puy[a)], Joan Cecilia[b)], Pablo Lodeiro[c)] and Francesc Mas[d)],

[a)]*Departament de Química,* [b)]*Dep Matemàtica. Universitat de Lleida, Rovira Roure 191, 25198 Lleida, Spain*

[c)]*Departamento de Química Física e Enxeñería Química I, Universidade da Coruña, Campus da Zapateira s/n 15071 A Coruña, Spain*

[d)]*Departament de Química Física and IQTC, Universitat de Barcelona, Martí i Franquès,1, 08028 Barcelona, Spain*

* corresponding author: jpuy@quimica.udl.cat

Abstract

Information on the Pb and Cd binding to a purified Aldrich Humic Acid (HA) is obtained from the influence of different fixed total metal concentrations on the acid-base titrations of this ligand. NICA (Non-Ideal Competitive Adsorption) isotherm has been used for a global quantitative description of the binding, which has then been interpreted by plotting the Conditional Affinity Spectra of the H^+ binding at fixed total metal concentrations (CAScTM). This new physicochemical tool, here introduced, allows the interpretation of binding results in terms of distributions of proton binding energies. A large increase in the acidity of the phenolic sites as the total metal concentration increases, especially in presence of Pb, is revealed from the shift of the CAScTM towards lower affinities. The variance of the CAScTM distribution, which can be used as a direct measure of the heterogeneity, also shows a significant dependence on the total metal concentration. A discussion of the factors that influence

the heterogeneity of the HA under the conditions of each experiment is provided, so that the smoothed pattern exhibited by the titration curves can be justified.

Keywords: macromolecular complexation, affinity spectrum, trace metal speciation, NICA

1. Introduction

Natural organic matter (NOM) plays a key role in the circulation of trace metal ions in the environment (Buffle, 1988;Ruzic, 1996). Accordingly, methods to quantify the speciation and to reach a deeper understanding of the characteristics of such complexation are of great interest. A strategy widely used for the quantitative description of the binding data relies on fitting the data to competitive isotherms. In the context of environmental systems, two of such isotherms are NICA (Non-Ideal Competitive Adsorption) isotherm, developed by Koopal, van Riemsdijk and coworkers (Benedetti et al., 1995;Kinniburgh et al., 1999;Koopal et al., 1994;van Riemsdijk et al., 1986) and Model V / VI,(Tipping, 2002;Tipping, 1998;Tipping and Hurley, 1992) which use a discrete set of binding affinities.

The knowledge of the affinity distributions underlying the different isotherms can help in the understanding of the binding characteristics of the organic matter. In an early paper (Sips, 1948), Sips reported an analytical expression for the inversion of monocomponent isotherms. However, its use has been rather limited up to now, probably because the cation binding to environmental ligands is essentially competitive. The analysis of the multidimensional distributions underlying competitive isotherms is even scarcer. Numerical regularization or approximate semianalytical techniques have been applied to solve this problem (Rusch et al., 1997) and recently, a general analytical expression for the affinity spectrum underlying competitive isotherms has been reported

(Garcés et al., 2004). The practical success of this methodology is at the end limited by the restrictive conditions for the existence of the affinity spectrum. For instance, the concept of multidimensional affinity spectrum cannot be used when metal and proton do not share the same complexation sites (as in the case of chelate complexation). In the case of the NICA model, the existence of multidimensional spectrum requires a common n_i value for all the competing ions, which is a hard restriction in most of the experimental data sets.

A step to overcome this limitation was the introduction of the conditional affinity spectrum (CAS) (Garcés et al., 2006). The CAS, which can be seen as a generalization of the conditional stability constant, is a less restrictive formalism since it focuses only on monodimensional distributions. For instance, it is not necessary that all cations share common sites for the existence of the CAS. As it was introduced, the CAS characterizes the affinity distribution for a given ion at fixed free concentration of all other competing ions. Applications to simple competitive systems as well as to complex natural media have been reported (Companys et al., 2007b;Puy et al., 2009;Puy et al., 2008;Rey-Castro et al., 2009). For the simplest case of only two kinds of ions (e.g., proton and a metal cation) as competitive binding agents, the experimental data obtained from metal titrations at fixed pH can be straightforwardly fitted to a competitive isotherm. Since a fixed pH reduces the competitive isotherm to a monocomponent one for the metal ion, the Sips inversion formula can then be applied for the computation of the CAS, which allows a relatively simple discussion of the metal-NOM binding properties.

However, other experimental strategies can be of interest. Among them, let us discuss the arrangement of acid base titrations performed in the presence of a constant total metal concentration, which is varied over successive experiments (Ephraim et al., 1986;Mathuthu and Ephraim, 1995;van Dijk, 1971). In addition to its experimental

simplicity, this procedure allows the indirect assessment of the binding characteristic of the competing cations by means of their effect on the proton binding. It can be shown that the constraint of constant total metal concentration reduces the competitive isotherm that describes the proton-NOM binding in the presence of metal ions to an effective monocomponent isotherm. Accordingly, the inversion formula of Sips can also be applied to the computation of the CAS of the NOM for the proton binding at different total metal concentrations, this allowing a simple discussion of the experimental results. The resulting conditional affinity spectra will be labeled simply as CAS or as CAScTM (when more specificity is needed). Obviously, the application of this procedure is not restricted to proton binding. Other cations can play the role of protons and be used to obtain indirect information about the binding characteristics of another metal whose total concentration is kept constant along the titration (Tipping et al., 2002).

The aim of this work is to use proton titration data of a purified Aldrich Humic Acid obtained at different total Cd and Pb concentrations to quantify the complexation of these ions to HA by means of the NICA isotherm. After the fitting of the binding data to the isotherm equation, Section 3 is devoted to the calculation of the CAScTM for the different total metal concentrations used in the experiments. Section 4 is devoted to the discussion of the CAScTM results and their comparison with the CAS corresponding to fixed free metal concentration, previously reported (Puy et al., 2008). Finally, the distribution of occupied sites is reported.

2. Materials and methods

2.1. Reagents and instrumentation

Humic acid (H1, 675-2; Aldrich) was purified following the procedure outlined elsewhere (Companys et al., 2007b;Companys et al., 2007a). Potassium nitrate was used as inert supporting electrolyte and prepared from solid KNO_3 (Fluka, Trace Select). Lead and cadmium solutions were prepared from the solid nitrate product (Merck, analytical grade). 0.1M standard aqueous solutions of HNO_3 or KOH (Ridel-de-Haën, Standard solution) were used in the titrations. Ultrapure water (Milli-Q plus 185 System, Millipore) was employed in all the experiments. Purified water-saturated nitrogen was used for deaeration.

pH was monitored with a glass electrode (Metrohm 6.0133.100) attached to an Orion Research 720A ion analyzer. Free Pb^{2+} and Cd^{2+} concentrations in solution were measured potentiometrically using the corresponding Ion Selective Electrodes (ISE) (namely, Metrohm 6.05020.170 Pb-ISE and Metrohm 6.05020.170 Cd-ISE, respectively). The same reference electrode Ag/AgCl/3 $mol.L^{-1}$ KCl, with a 0.1 $mol.L^{-1}$ KNO_3 jacket (Metrohm 6.0726.100) was used for the pH electrode and metal ISE. The pH electrode was previously calibrated in terms of proton concentration, c_H (rather than activity) following Gran's method (Gran, 1952) at the same ionic strength used in the HA titrations. Routine calibrations of the metal ISE were performed with total metal concentrations ranging from $1x10^{-6}$M to $5x10^{-4}$M in 0.1M KNO_3 at pH4.

The potentiometric measurements were carried out coupling the Orion pH/ISE meter with a Metrohm Dosimat dispenser. The entire titration setup was controlled by a homemade program running on a personal computer. The samples were placed in a double-walled potentiometric glass cell thermostated at 25ºC. N_2 bubbling and soda lime traps were used throughout to prevent CO_2 contamination. The potential between

the work electrode (pH or ISE) and the reference electrode was measured and recorded after a drift criterion of <0.1mV/min has been achieved.

All the proton titrations (in absence and in the presence of metal) were performed with a solution initially containing 0.45g·L^{-1} of HA in 0.1M KNO_3 after pH was cycled up to 7.0 and back to pH 3.5 to avoid hysteretic effects (Milne et al., 1995). Proton titrations in presence of metal were performed at fixed total metal concentration of $c_{T,M} = 10^{-5}$M, 10^{-4}M, 3.16x10^{-4}M, 5x10^{-4}M, 7.5x10^{-4}M and 10^{-3}M in the lead experiments and $c_{T,M} = 10^{-5}$M, 10^{-4}M, 5x10^{-4}M, 10^{-3}M and 3x10^{-3}M in the cadmium experiments.

The raw titration data consist of sets of E(mV) vs. v(KOH) data which were converted into -log c_H vs. v(KOH) data by means of the calibration curves (Nernst equation).

Let Q_H and $Q_{max,H}$ denote, respectively, the current and maximum possible concentration of protonated sites (i.e. the current and maximum moles of protonated functional groups per kg of HA). In the absence of metal, there are no proton sites occupied by metals and $Q_{max,H} - Q_H$ stands for the free acid sites of the humic acid. Otherwise, $Q_{max,H} - Q_H$ stands for the proton sites (mol.kg^{-1}) not occupied by protons. Let Q_M stand for the moles of M bound to a kg of humic acid. Assuming that all the free proton sites are negatively charged (since amino and other positively charged groups are usually minor sites in HA), then the absolute value of the macromolecular charge can be written as $Q_{max,H} - Q_H - 2Q_M$, which holds for any arbitrary stoichiometric relationship between metal M and proton groups. Thus, the charge balance reads

$$\left(Q_{max,H} - Q_H - 2Q_M\right)c_{HA} + c_{OH^-} + c_{NO_3^-} = c_{H^+} + c_{K^+} + 2c_{M^{2+}} \quad (1)$$

where c_{HA} is the concentration of humic acid in kg L^{-1}, and the rest of the concentrations c_i are in mol L^{-1}. The charges of the ions will be omitted in the following, for clarity reasons.

Using $c_{NO_3} = c_{KNO_3} + 2c_{T,M}$, simple algebraic manipulation of Eqn. (1) shows that $Q_{max,H} - Q_H$ can be computed as:

$$Q_{max,H} - Q_H = \frac{c_H + c_{KOH} - \frac{K_W}{c_H}}{c_{HA}} \quad (2)$$

Expression (2) allows the conversion of the $-\log c_H$ vs. v(KOH) (volume of added base) data into $Q_{max,H} - Q_H$ vs. $-\log c_H$ data.

2.2. Fitting of the binding data to the NICA Isotherm

Using glass electrode measurements exclusively

Proton titration data of the HA in absence of metal show a double wave shape (see Fig. 1a). Accordingly, bimodal distributions have been used to describe the proton binding. Let $Q_{max,H,1}$ and $Q_{max,H,2}$ be the total moles of proton sites per kg of HA in the corresponding modal distribution. As $Q_{max,H} - Q_H$ represents the amount of humic functional groups that are not protonated, then

$$Q_{max,H} - Q_H = \left(Q_{max,H,1} + Q_{max,H,2}\right) - Q_H = Q_{max,H,1}(1 - \theta_{H,1}) + Q_{max,H,2}(1 - \theta_{H,2}) \quad (3)$$

Here, NICA will be used to describe the binding. Although the binding energy can be split into an electrostatic component and a chemical or intrinsic one, we will analyze here the raw binding data (i.e. without performing any polyelectrolytic correction). The resulting NICA parameters will then be conditional to the ionic strength of the medium, i.e. 0.1M KNO_3.

According to NICA isotherm, $\theta_{H,i}$ in eqn. (3) (with *i*=1 for the carboxylic distribution and *i*=2 for the phenolic one) is given by

$$\theta_{\mathrm{H},i} = \frac{Q_{\mathrm{H},i}}{Q_{\max,\mathrm{H},i}} = \frac{\left(\bar{k}_{\mathrm{H},i}\, c_{\mathrm{H}}\right)^{n_{\mathrm{H},i}}}{\left(\bar{k}_{\mathrm{H},i}\, c_{\mathrm{H}}\right)^{n_{\mathrm{H},1}} + \left(\bar{k}_{\mathrm{M},i}\, c_{\mathrm{M}}\right)^{n_{\mathrm{M},i}}} \frac{\left(\left(\bar{k}_{\mathrm{H},i}\, c_{\mathrm{H}}\right)^{n_{\mathrm{H},i}} + \left(\bar{k}_{\mathrm{M},i}\, c_{\mathrm{M}}\right)^{n_{\mathrm{M},i}}\right)^{p_i}}{1+\left(\left(\bar{k}_{\mathrm{H},i}\, c_{\mathrm{H}}\right)^{n_{\mathrm{H},i}} + \left(\bar{k}_{\mathrm{M},i}\, c_{\mathrm{M}}\right)^{n_{\mathrm{M},i}}\right)^{p_i}} \tag{4}$$

indicating that the proton coverage of the sites of a given distribution depends also on the free metal concentration, c_{M}, as resulting from the competitive binding between both cations. $\bar{k}_{j,i}$, $n_{j,i}$, and p_i are parameters of the isotherm that characterize the proton and metal binding to the HA within the NICA model. They can be obtained from the fitting of the experimental values of $Q_{\max,\mathrm{H}}$-Q_{H} *vs.* pH to the NICA isotherm by means of Eqns. (2)-(4).

However, the use of eqn. (4) requires the knowledge of free metal concentration at each pH. In absence of specific metal ISE measurements, the concentration of the free species is calculated from the total concentration, through the mass balance:

$$c_{\mathrm{M}} = c_{\mathrm{T,M}} - c_{\mathrm{HA}} Q_{\mathrm{M}} \tag{5}$$

where Q_{M} is given, within the NICA model, by

$$Q_{\mathrm{M}} = Q_{\max,\mathrm{H},1} \frac{n_{\mathrm{M},1}}{n_{\mathrm{H},1}} \frac{\left(\bar{k}_{\mathrm{M},1} c_{\mathrm{M}}\right)^{n_{\mathrm{M},1}}}{\left(\bar{k}_{\mathrm{H},1} c_{\mathrm{H}}\right)^{n_{\mathrm{H},1}} + \left(\bar{k}_{\mathrm{M},1} c_{\mathrm{M}}\right)^{n_{\mathrm{M},1}}} \frac{\left(\left(\bar{k}_{\mathrm{H},1} c_{\mathrm{H}}\right)^{n_{\mathrm{H},1}} + \left(\bar{k}_{\mathrm{M},1} c_{\mathrm{M}}\right)^{n_{\mathrm{M},1}}\right)^{p_1}}{1+\left(\left(\bar{k}_{\mathrm{H},1} c_{\mathrm{H}}\right)^{n_{\mathrm{H},1}} + \left(\bar{k}_{\mathrm{M},1} c_{\mathrm{M}}\right)^{n_{\mathrm{M},1}}\right)^{p_1}} + \\ + Q_{\max,\mathrm{H},2} \frac{n_{\mathrm{M},2}}{n_{\mathrm{H},2}} \frac{\left(\bar{k}_{\mathrm{M},2} c_{\mathrm{M}}\right)^{n_{\mathrm{M},2}}}{\left(\bar{k}_{\mathrm{H},2} c_{\mathrm{H}}\right)^{n_{\mathrm{H},2}} + \left(\bar{k}_{\mathrm{M},2} c_{\mathrm{M}}\right)^{n_{\mathrm{M},2}}} \frac{\left(\left(\bar{k}_{\mathrm{H},2} c_{\mathrm{H}}\right)^{n_{\mathrm{H},2}} + \left(\bar{k}_{\mathrm{M},2} c_{\mathrm{M}}\right)^{n_{\mathrm{M},2}}\right)^{p_2}}{1+\left(\left(\bar{k}_{\mathrm{H},2} c_{\mathrm{H}}\right)^{n_{\mathrm{H},2}} + \left(\bar{k}_{\mathrm{M},2} c_{\mathrm{M}}\right)^{n_{\mathrm{M},2}}\right)^{p_2}} \tag{6}$$

Eqns. (5) and (6) can be used to obtain c_{M}, which, replaced in (4), allows to compute θ_{H} and $Q_{\max,\mathrm{H}}$-Q_{H} for a given pH, $c_{\mathrm{T,M}}$ and a given set of NICA parameters. The comparison of the calculated $Q_{\max,\mathrm{H}}$-Q_{H} value with the experimental one given in (2) allows the fitting of the NICA parameters.

Due to the high number of unknown parameters included in the model, the particular procedure followed to obtain the best-fit values from experimental data deserves further comment. In a first stage, a least-squares fit of the six parameters $Q_{\max,\mathrm{H},i}$, $\bar{k}_{\mathrm{H},i}$, $m_1 = n_{\mathrm{H},1} \times p_1$ and $m_2 = n_{\mathrm{H},2} \times p_2$ was carried out using just the proton binding data in absence of metal. However, this titration curve is barely informative about the three parameters of the second distribution (See below, in section 4.1, for a more detailed discussion). Therefore, in a second stage, the fitted values of $\bar{k}_{\mathrm{H},1}$; $n_{\mathrm{H},1} \times p_1$; and $Q_{\max,\mathrm{H},1}$ obtained in the first step were kept fixed while the rest of proton parameters as well as the whole set of metal parameters (e.g. $\bar{k}_{\mathrm{M},1}$, $n_{\mathrm{M},2}$, etc.) were fitted using all the experimental data together (including titrations in presence of Pb/Cd). In this way the reliability of the fitted parameters associated to the second modal distribution is improved and more robust values of the ion-independent parameters of the HA (such as $Q_{\max,\mathrm{H},i}$ and p_i) are obtained.

Using both glass electrode and metal ISE measurements

The above fitting procedure does not require the use of experimental values of c_{M}. In this way, the metal binding information is obtained indirectly from its influence on the proton titration curves using glass electrode data only. Therefore, this method can be used to study competition effects due to metals for which ISE are not commercially available.

In order to check the accuracy of this methodology, an alternative fitting strategy is performed. In this case, we use the direct experimental c_{M} values measured with the metal ISE instead of estimating c_{M} by solving Eqns. (5) and (6). The procedure is now straightforward: the values of θ_{H}, as given by Eqn. (4), are computed from the

experimental c_M and c_H values using a trial set of NICA parameters. Eqn. (3) then allows the computation of $Q_{max,H}$-Q_H which are compared with the experimental titration values leading to the fitting of the NICA parameters for proton and metal. Hence, this second procedure makes use of all the experimental information available.

3. Conditional affinity spectra at constant total metal concentration

An interesting physicochemical tool for the interpretation of the binding data is based on the use of a distribution of independent sites with different intrinsic affinities and abundances. Using this strategy, the coverage can be thought as the superposition of coverages to the different kinds of sites.

Recent work (Garcés et al., 2006) has developed the concept of conditional affinity spectrum (CAS). Indeed, by fixing c_H, a two-component isotherm becomes monocomponent, with the subsequent monodimensional affinity spectrum indicating the effective affinity distribution seen by the metal at the pH considered. As these distributions are pH dependent, we call them conditional affinity spectra. Analytical expressions of the CAS underlying NICA isotherm have been reported as well as expressions for the dependence of the main parameters of this distribution (average and variance) with respect to pH (Puy et al., 2009;Rey-Castro et al., 2009). Notice that the use of the analytical expressions of the CAS underlying NICA overcomes the limitations due to the possible presence of artefacts in the CAS obtained by direct numerical inversion of experimental binding data (Dzombak et al., 1986;Merz, 1980;Vos and Koopal, 1985).

Here, we aim at extending the CAS concept to another situation of experimental interest: the proton titration at fixed total metal concentration. By fixing the total metal

concentration, we will have an additional equation that can be used to eliminate the dependence of the proton coverage on the metal concentration, so that a competitive isotherm is transformed into a formally monocomponent one. The inversion formula for monocomponent isotherms can, then, be applied. The resulting conditional affinity spectrum, which will be labelled as CAScTM, will indicate the distribution of sites with a given affinity *for the proton* under the restriction of fixed total metal concentration. Notice that all the sites of the macromolecule (and not just the free ones) are available for the proton, but with a reduced affinity (metals have to be extracted prior to proton binding). The existence of the CAScTM is not guaranteed, since there is no analytical inversion of the NICA isotherm under constant $c_{T,M}$ conditions. There might arise concentrations and NICA parameters for which there was no CAScTM. Mathematical sufficient conditions for the existence of the affinity spectrum are the recovering of the binding curve from the CAS

$$Q_H = Q_{max,H} \int_{-\infty}^{\infty} p\left(\log k_H^{'}, c_{T,M} = cnt\right) \frac{k_H^{'} c_H}{1 + k_H^{'} c_H} d \log k_H^{'} \qquad (7)$$

and the normalization condition of the affinity distribution, which has to be semi-definite positive. In all the cases shown below (Figs. 4-7) we have checked that from the resulting CAScTM, the binding curve is recovered and that the integration of the CAScTM reaches the expected value.

Obviously, the use of the CAScTM is not restricted to protons in a system with only one metal, but it can be straightforwardly extended to any probed ion whose free (or bound) concentration was easily measured in a general system when fixing the total concentration of the rest (Tipping et al., 2002).

The inversion formula that gives the affinity spectrum in monocomponent adsorption is (Koper and Borkovec, 1996a):

$$p\left(\log k'_{\mathrm{H}}; c_{\mathrm{T,M}} = \mathrm{cnt}\right) = \frac{\ln(10)}{\pi}\left|\mathrm{Im}\left[\theta_{\mathrm{H}}\left(c_{\mathrm{T,M}} = \mathrm{cnt}, c_{\mathrm{H}} = -1/k'_{\mathrm{H}}\right)\right]\right| \quad (8)$$

where Im means "take the imaginary part", the prime in k'_{H} labels a conditional affinity value and cnt is the abbreviation for constant. According to (8), for a given k'_{H}, the corresponding density of sites $p\left(\log k'_{\mathrm{H}}; c_{\mathrm{T,M}} = \mathrm{cnt}\right)$, is obtained by using $c_{\mathrm{H}} = -1/k'_{\mathrm{H}}$ in the calculation of the proton coverage.

The overall proton coverage is given by

$$\theta_{\mathrm{H}} = \frac{Q_{\mathrm{max,H,1}}}{Q_{\mathrm{max,H,1}} + Q_{\mathrm{max,H,2}}}\theta_{\mathrm{H,1}} + \frac{Q_{\mathrm{max,H,2}}}{Q_{\mathrm{max,H,1}} + Q_{\mathrm{max,H,2}}}\theta_{\mathrm{H,2}} \quad (9)$$

where $\theta_{\mathrm{H},i}$ is given by (4). However, Equation (9) cannot be used directly in (8) without introducing the restriction of fixed total metal concentration. Actually, $\theta_{\mathrm{H},i}$ as given by (4) depends on both c_{M} and c_{H}. Thus, we have to express c_{M} in terms of c_{H} and $c_{\mathrm{T,M}}$ before using $c_{\mathrm{H}} = -1/k'_{\mathrm{H}}$. Eqns. (5) and (6) allow, for a given c_{H} and $c_{\mathrm{T,M}}$, the computation of c_{M}, which replaced in (9) and (8) yields $p\left(\log k'_{\mathrm{H}}; c_{\mathrm{T,M}} = \mathrm{cnt}\right)$. The software Octave (Eaton, 2010), which uses complex numbers in the solution of a system of equations, has been used for the numerical inversion of the monocomponent isotherm

4. Results and discussion

4.1. Binding results.

NICA description using glass electrode data

The proton binding data obtained in absence of added metal are depicted in Fig. 1. Results from several independent titration experiments performed over different sub-samples of the same purified HA stock solution are plot together in order to give an idea of the repeatability achieved. Note the poor reliability of the data above pH 10. Figure 1

also depicts the results calculated using NICA isotherm with the fitted parameters reported in Table 1, which were obtained as described in Section 2.2. The agreement with experimental data is fairly good and deviations are usually within experimental error.

Fig. 1 also displays the values calculated for every modal distribution separately, in order to assess the relative amount of charge associated with each distribution. Notice that the fitted value of $Q_{max,1} + Q_{max,2}$ is 7.6 mol/kg, which goes beyond the region of $Q_{max,H} - Q_H$ were the data is well reproducible (i.e., up to ca. 5 mol/kg, see Fig 1). Fig. 1 also shows that the 7.6-5=2.6 mol/kg of sites outside the experimental window of Fig. 1 belong to the phenolic distribution, whose charge is increasing within the pH range 9-11. It could, then, be expected that the parameters of the phenolic distribution would suffer an important uncertainty, if proton binding parameters were obtained from Fig. 1 only. To mitigate this problem, the fit of the phenolic distribution has been carried out using data obtained in presence of metal ions (figures 2-4), as indicated in Section 2.2. Under these conditions, $Q_{max,H} - Q_H$ reaches values close to 7 in presence of lead at the highest concentration (see Fig. 2) and close to 6 for the case of Cd (See Fig. 3). These $Q_{max,H} - Q_H$ values are much closer to the fitted value of $Q_{max,1} + Q_{max,2}$ (i.e. 7.6 mol/g) giving confidence to this value as well as to the other proton distribution parameters. Metal ions release protons from acidic groups too weak to be ionized otherwise, as already reported by Ephraim et al.(Ephraim et al., 1986;Mathuthu et al., 1995)

The distribution of affinities resulting from the fitted NICA parameters is depicted in Fig.1b. Since NICA reduces to a Langmuir-Freundlich isotherm when only one ion is present in the system, the distribution depicted in Fig. 1b is a bimodal Sips distribution (Puy et al., 2009). The first peak of this distribution is centered at log ($\bar{k}_{H,1}$ / M^{-1})=4.59

and is usually associated with the "carboxylic" type of sites, whereas the second peak (the "phenolic" distribution) is centered at log ($\bar{k}_{H,1}$ / M^{-1})=11.02, and has a smaller area (which reflects the relative values of $Q_{max,H,1}$ and $Q_{max,H,2}$). The width of every distribution indicates the binding heterogeneity of the corresponding sites, and it depends on $m_i = n_{H,i} \times p_i$. The global distribution characterizes the overall H binding to the HA.

Figs. 2 and 3 depict the titration data in presence of metal. As can be seen, for a fixed pH, a larger amount of metal decreases Q_H (via competition) and, consequently, $Q_{max,H}$ - Q_H increases. The decrease of Q_H indicates that the presence of metal (Pb or Cd) facilitates the deprotonation, i. e., increases the acidity of the HA by reducing the effective proton binding affinity since an increasing part of the binding energy has to be invested in extracting the metals. The influence of the metal concentration is higher in the case of Pb than in the case of Cd, especially below pH 7.

Theoretical values of ($Q_{max,H}$ - Q_H) for each modal distribution, as computed from the NICA parameters reported in Table 1, are also depicted in Figures 2 and 3. The agreement with experimental data is quite good, which supports the assumption that accurate information on Pb or Cd binding to HA can be obtained indirectly from the proton binding data. From the data displayed in Fig. 2, it can be observed that the deprotonation of the phenolic sites in the presence of Pb takes place at lower pH values (above 4.5, see dashed curves) than in the presence of Cd. In the latter case, the titration of "phenolic" sites does not start until pH 6.5 (see Fig. 3). Therefore, when Pb is present, both distributions (carboxylic and phenolic) compete for the binding with protons at most pH's (notice, in Fig 2, that the phenolic sites represent eventually up to one third of the total amount of titrated groups). On the contrary, in the case of Cd, the

protonation of the phenolic distribution takes place mainly at a higher range of pH than the carboxylic distribution (i.e. the deprotonation of carboxylic and phenolic groups is more sequential). Since the sites of the HA are the same in all the cases (Figs. 1, 2 or 3), the change of the acidity of these sites in every figure reflects how the conditional value of the acidity depends on the composition of the system. This dependence cannot be straightforwardly quantified in heterogeneous systems, since it depends on the binding affinity of the metals present, the stoichiometry of the H/M exchange and the correlation of the binding energies of the different competing ions (Puy et al., 2008;Puy et al., 2009). However, the observed effect can be used to obtain information on these phenomena as discussed below.

Notice that the effect of hydrolysis, that could be especially important for Pb, has not been taken into account in the fitting procedure. The precipitation of solid species under equilibrium conditions was excluded, since the product of ionic concentrations $Q_{sp} = c_{Pb^{2+}} c_{OH^-}^2$, calculated from experimental pH and Pb-ISE data throughout the titrations is not constant (See Fig. EA-1 in the Electronic Annex). On the other hand, a simple speciation calculation using VMINTEQ indicates a non-negligible concentration of aqueous species $Pb(OH)^+$ and $Pb_3(OH)_4^{2+}$ at 7.5 < pH < 9. In principle, these species could also bind to the HA (Milne et al., 2003), but, for the sake of simplicity, no specific set of NICA parameters have been considered for them. Therefore, the NICA parameters reported in Table 1 or 2 have to be considered as "effective" for the mixture of Pb aqueous species.

NICA description using both glass and metal ISE data

As indicated in section 2.2, a second NICA description of the binding data was performed using, in this case, the free metal concentrations recorded with the ISE along the proton titrations depicted in Figs. 2 and 3. The fitted parameters are reported in

Table 2, while the figures showing the experimental and predicted $Q_{max,H}$ - Q_H values are included in the Electronic Annex (Fig. EA-2 and EA-3). The agreement between calculated and measured values is similar to that shown in Fig. 2 and 3 and the differences between both sets of parameters (Table 1 and 2) are not significant. These results confirm the feasibility of using the glass electrode as an indirect probe for the quantitative description of the metal binding.

4.2. Conditional affinity spectra of H-HA at fixed total Pb or Cd concentrations

The CAScTM of proton binding to HA in presence of different total amounts of Pb and Cd, computed as indicated in Section 2.2, are depicted in Figures 4 and 5, respectively. The plotted distributions offer a visual interpretation of the influence of the metal on the proton affinity of the ligand in experiments performed at constant $c_{T,M}$.

Let us first compare these spectra (Figs. 4 and 5) with the affinity distribution in absence of competing metal ion (Fig. 1b). It is clear that an increasing amount of metal induces a shift in the affinity of the proton sites towards progressively lower values. This shift reflects the decrease in the effective proton binding energy, due to the work that has to be expended in removing the metal bound to the proton sites. However, this shift is not constant along the affinity axis, and therefore the global shape of the spectra changes. Three main mechanisms are responsible for the changes in shape of the CAScTM: i) the distance between carboxylic and phenolic modes is affected by the different sensitivity of each modal distribution to an increase in $c_{T,M}$; ii) the value of the free concentration of the competing species, c_M, is not constant throughout a proton titration carried out at a fixed $c_{T,M}$; and iii) the effect of a particular value of c_M depends on the “correlation” (in a broad sense) between the binding energies of proton and metal ions. For a general case where both cations do not necessarily share common

sites, a positive correlation (in a broad sense) means that sites with stronger affinity for protons are mainly involved in the sites with stronger affinity for the metal ions.

The mechanisms above mentioned deserve further comments. The first noticeable feature in the evolution of the CAScTM shape is that the distance between the two modal distributions decreases as the Pb/Cd concentration increases (see Figs. 4 and 5). Therefore, the variance of the overall CAScTM tends to decrease, which means that the HA behaves globally as a less heterogeneous ligand (see, for instance, the larger slope of proton titrations at the highest Pb concentration in Fig 2). This is a result of the impact of the metal ion being larger on the phenolic distribution than on the carboxylic one. This effect is especially remarkable in the case of Pb, where the two peaks of the corresponding modal distributions are significantly overlapped. The stronger shift of the phenolic mode in the presence of Pb (compared to Cd) is due to the larger value of log ($\overline{k}_{\mathrm{Pb},2}$ / M^{-1}) in comparison with log ($\overline{k}_{\mathrm{Cd},2}$ / M^{-1}). Recall that log ($\overline{k}_{i,2}$ / M^{-1}) indicates the average binding energy when only ion *i* is present in the system, so that it indicates the energy expended by the proton to extract the metal in each case.

On the other hand, it can be observed that the phenolic affinity distribution broadens in the presence of metal at relatively low concentrations (see e.g. figs. 4a, 4b, 5a and 5b). Accordingly, smoothed titration curves around the second equivalence point appear at low metal concentrations (compare the phenolic titration curves depicted in red in Figs. 2 or 3 with Fig. 1a). It can also be observed that, as the phenolic peak broadens, a double peaked shape appears (see figs. 4a and 4b for the Pb case and 5a for the Cd case).

The broadening of a modal distribution can be explained in terms of the last two mechanisms mentioned above. Let us first consider a case where proton and metal share the same sites, with affinities k_{H} and k_{M}, respectively. In this case, the effective proton

binding affinity of a site, $k_{\mathrm{H}}^{'}$, in the presence of a concentration c_{M} of the competing ion is given by (Puy et al., 2009)

$$\log k_{\mathrm{H}}^{'} = \log k_{\mathrm{H}} - \log\left(1 + k_{\mathrm{M}} c_{\mathrm{M}}\right) \tag{10}$$

where k_{H} would represent the binding affinity in absence of metal. If the concentration of the free competing ion was kept fixed, then the conditional affinity $k_{\mathrm{H}}^{'}$ would also remain constant. But, under conditions of constant $c_{\mathrm{T,M}}$, this is no longer true. Instead, the value of c_{M} will vary along the titration within the range $0 \le c_{\mathrm{M}} \le c_{\mathrm{T,M}}$, depending on the occupation of protons, the proton/metal exchange ratio and the concentration of ligand. Therefore, the total number of sites with intrinsic affinities (k_{H}, k_{M}) will be distributed (i.e. "split" or "scattered"), in the CAScTM, into different abundances of a certain range of effective affinities. For instance, when protons bind to a langmuirian site, they displace metals into the solution and consequently increase c_{M}, which, according to Eqn. (10), modifies (decreases) the effective proton affinity of the site.

In a general case, a given proton site (characterized by a value of k_{H}) may display a wide or narrow range of intrinsic binding affinities for the metal ion, k_{M}, depending on the degree of correlation between the binding energies of both ions. Consequently, every kind of proton sites will "scatter" into a range of effective binding affinities in the presence of metal ions. As discussed previously (Puy et al., 2009) for spectra at constant c_{M}, this correlation influences the width of the affinity distribution when $c_{\mathrm{T,M}}$ changes. In absence of correlation, k_{M} is independent of k_{H}, which means that a given site may display many possible values of k_{M}, and therefore the scattering is large. Conversely, in presence of strong correlation, this scattering is less significant, since sites with high k_{H}

values tend to show only high k_M values (positive correlation) so the shift in the effective affinity has a precise value, given by Eqn. (10).

In summary, due to the variable contribution of $k_M c_M$ to the binding of protons, the shift in the effective binding affinity of each site in the presence of metal ions is not necessarily constant throughout the $\log k_H^{'}$ axis. In practice, the spectra of a given modal distribution (most noticeably, the phenolic one) are relatively broad at low metal concentrations, due to the competition effects already mentioned, but become narrower at large metal concentrations. Indeed, as the metal concentration increases, the variation of the free metal concentration along the proton titration is less relevant, the heterogeneity associated to this phenomenon decreases and the correlation becomes more important. At very high $c_{T,M}$, NICA becomes a Langmuir-Freundlich isotherm with exponent n_H:

$$\theta_H\left(c_M \to \infty, c_H\right) = \frac{\left(\frac{\overline{k}_H}{\left(\overline{k}_M c_M\right)^{\frac{n_M}{n_H}}} c_H\right)^{n_H}}{1+\left(\frac{\overline{k}_H}{\left(\overline{k}_M c_M\right)^{\frac{n_M}{n_H}}} c_H\right)^{n_H}} \tag{11}$$

and the phenolic distribution at high metal dosage becomes symmetric, centered at $\log \overline{k}_H - \frac{n_M}{n_H}\log\left(\overline{k}_M c_M\right)$ with variance given by (Puy et al., 2009)

$$\sigma^{'2}_{c_M \to \infty} = \frac{\pi^2}{\left(\ln 10\right)^2}\frac{1-{n_{H,2}}^2}{3{n_{H,2}}^2} \tag{12}$$

which is independent from the metal present. For the current case (Pb or Cd systems) $\sigma^{'2}_{c_M \to \infty} = 0.16$, a small value determined by the high $n_{H,2}$ obtained.

The change of the variance of the phenolic distribution with increasing $c_{T,M}$ is the responsible for the change of the slope of the titration curve of the phenolic distribution depicted in Figs. 2 and 3. A higher variance indicates elongated titration curves, while a lower variance indicates a sharper increase of the titration curve.

Figures 4 and 5 also depict in shaded area the fraction of sites of each affinity value $k_H^{'}$ that are occupied (protonated) at pH = 8, calculated as $p\left(\log k_H^{'}, c_{T,M} = cnt\right)\frac{k_H^{'}c_H}{1+k_H^{'}c_H}$.

Notice that although pH=8 in all the figures, the increase of metal concentration reduces the shaded area, since the affinity for the protons decreases.

The preceding discussion can be generalized to other cases including complex mixtures of metals. The shift of the phenolic and carboxylic proton affinity distributions, as well as the effective heterogeneity, will be dependent on the concentrations of all the metals and ligands present. The final spectrum of the HA can exhibit both distributions (carboxylic and phenolic) being overlapped or even inverted depending on the concentration of metals present and on the affinity parameters shown by each distribution (Rey-Castro et al., 2009)

Since we used conditional NICA parameters obtained in 0.1M KNO_3, the spectra displayed in this section include the electrostatic contribution to the binding energy. The extent of this contribution may not be constant during the titration, given that the electrostatic charge of the macromolecule varies as a function of the proton and metal coverage. Therefore, the conditional affinity spectra reported here correspond to an effective distribution of independent uncharged sites that gives rise to the same binding curve as the experimental system, although these sites do not necessarily correspond to actual sites, in a chemical sense. The electrostatic effect is not the only phenomenon that leads to such situation. For instance, a ligand having identical and independent sites

only (Langmuirian adsorption) behaves like a heterogeneous ligand for the competitive binding of protons and metal ions under the constraint of constant $c_{T,M}$, since the free metal concentration, and consequently the effective site affinity, depends on the proton occupation, as was discussed above. A similar situation holds when the metal binding is multidentate, which can also be described through an equivalent heterogeneous distribution of independent sites (Garcés et al., 2006;Koper and Borkovec, 1996b). Notice also that, under the concentrations of metal and HA here used, larger than the usual in natural waters, some aggregation can occur so that the reported CAS include also this phenomenon.

Finally, in order to assess the uncertainty of the computed CAScTM, we plot in Fig. EA-4 the CAS for a total Pb concentration obtained with NICA parameters of Table 1 and Table 2. There is a clear qualitative agreement between both distributions although there are some quantitative differences due to the differences between the set of parameters used.

4.3. Comparison of the CAScTM with the CAScM

Further insight into the features of the CAScTM can be obtained by comparing these spectra with the CAS at constant free (instead of total) metal concentration, which we distinguish here with the label CAScM. In particular, it is interesting to compare with the CAScM obtained at the limiting cases where c_M has the lower and greater value in the concentration "window" covered through the experiments performed at constant total metal concentration.

An analytical expression for the CAScM underlying NICA isotherm and a discussion of the main characteristic of the binding in terms of the CAScM have been reported recently (Puy et al., 2009;Puy et al., 2008;Rey-Castro et al., 2009). For an easier

comparison, the CAScM (dashed-dotted line in Figs. 6 and 7) corresponding to a fixed c_M equal to the free metal concentration arising in the Pb or Cd systems at a very high pH (low free metal concentration) is plotted together with the CAScM corresponding to the c_M reached at the lowest pH value (highest free metal concentration) considered in the experimental titration (dashed line) and to the CAScTM (continuous line). Since both CAScM spectra at fixed c_M are well apart and correspond to situations covered by the fixed $c_{T,M}$ case, one can rationalize the higher heterogeneity of the CAScTM which integrates (among others) the two depicted extreme c_M conditions. Notice also that the CAScM represented by the dashed line in Figs. 6 and 7, corresponding to the highest free metal concentration in the titration depicted in Figs. 2 or 3, resembles the CAScTM of the highest $c_{T,M}$ value depicted in Fig. 4d or 5d as expected.

Conclusions

Proton titrations of HA have been conducted at fixed total metal concentrations. The binding parameters of NICA isotherm for both metal and proton ions, have been obtained from the impact of the metal on the proton titration curves.

The conditional affinity spectrum of the proton at fixed total metal concentrations (and fixed HA concentration), CAScTM, has been developed as a physicochemical tool for the interpretation of the binding results. The CAScTM distributions allow a complete characterization of: i) the conditional affinity seen by the proton at each total metal concentration, ii) the effective heterogeneity of the binding and iii) the distribution of occupied proton sites at a given concentration.

The presence of Pb/Cd mainly influences the phenolic distribution of the HA, which shifts towards lower affinities as $c_{T,M}$ increases. This shift justifies the increase of the acidity of the HA in presence of increasing metal concentrations.

Acid base titration curves of the HA at different total metal concentrations were quite elongated, indicating a high heterogeneity of the system. The variance of the CAScTM can be used to rationalise the heterogeneous behaviour of the HA. On one hand, the two modal distributions approach each other due to the larger shift of the phenolic distribution. However, the variance of the phenolic distribution is influenced by different phenomena, e.g. it initially increases as $c_{T,M}$ increases due to the range of c_M values arising in the system along the proton titration. Additionally, the variance can decrease as the metal concentration keeps increasing, if there is a high correlation between the binding energies of metal and proton. At high $c_{T,M}$ values, the variance is independent of the competing metal present and only dependent on the cation studied (in this case, protons) and the HA.

Acknowledgment

This work was financially supported by the Spanish Ministry of Education and Science (Projects CTQ2006-14385, CTM2006-13583, CTQ2009-07831 and CTQ2009-14612), from the "Comissionat d'Universitats i Recerca de la Generalitat de Catalunya" 2009SGR00465 and XRQTC. S. Mongin acknowledges a FPI fellowship from Ministerio de Educacion y Ciencia of Spain. P. Lodeiro gratefully acknowledges financial support from Xunta de Galicia through Ángeles Alvariño projects AA 10.02.56B.444.0 and 10.02.561B.480.0, both co-funded by European Social Funds.

References

Benedetti M. F., Milne C. J., Kinniburgh D. G., Vanriemsdijk W. H., and Koopal L. K. (1995) Metal-Ion Binding to Humic Substances - Application of the Nonideal Competitive Adsorption Model. *Environ. Sci. Technol.* **29**, 446-457.

Buffle J. (1988) Interpretation of complexation equilibria. In *Complexation Reactions in Aquatic Systems. An Analytical Approach.* Ellis Horwood Limited, Chichester, pp. 195-303.

Companys E., Garcés J. L., Salvador J., Galceran J., Puy J., and Mas F. (2007a) Electrostatic and specific binding to macromolecular ligands. A general analytical expression for the Donnan volume. *Colloids Surf. A* **306**, 2-13.

Companys E., Puy J., and Galceran J. (2007b) Humic acid complexation to Zn and Cd determined with the new electroanalytical technique AGNES. *Environ. Chem.* **4**, 347-354.

Dzombak D. A., Fish W., and Morel F. M. M. (1986) METAL HUMATE INTERACTIONS .1. DISCRETE LIGAND AND CONTINUOUS DISTRIBUTION MODELS. *Environ. Sci. Technol.* **20**, 669-675.

Eaton J. W. (2010) GNU Octave, a high-level language for numerical computations. http://www.octave.org.

Ephraim J., Alegret S., Mathuthu A., Bicking M., Malcolm R. L., and Marinsky J. A. (1986) A united physicochemical description of the protonation and metal-ion complexation equilibria of natural organic-acids (Humic and Fulvic Acids) .2. Influence of polyelectrolyte properties and functional-group heterogeneity on the protonation equilibria of Fulvic Acid. *Environ. Sci. Technol.* **20**, 354-366.

Garcés J. L., Mas F., and Puy J. (2004) Affinity distribution functions in multicomponent heterogeneous adsorption. Analytical inversion of isotherms to obtain affinity spectra. *J. Chem. Phys.* **120**, 9266-9276.

Garcés J. L., Mas F., and Puy J. (2006) Conditional equilibrium constants in multicomponent heterogeneous adsorption: The conditional affinity spectrum. *J. Chem. Phys.* **124**, 044710-1-14.

Gran G. (1952) Determination of the equivalence point in potentiometric titrations. Part II. *Analyst.* **77**, 661-671.

Kinniburgh D. G., van Riemsdijk W. H., Koopal L. K., Borkovec M., Benedetti M. F., and Avena M. J. (1999) Ion binding to natural organic matter: competition, heterogeneity, stoichiometry and thermodynamic consistency. *Colloids Surf. A* **151**, 147-166.

Koopal L. K., van Riemsdijk W. H., Dewit J. C. M., and Benedetti M. F. (1994) Analytical isotherm equations for multicomponent adsorption to heterogeneous surfaces. *J. Colloid. Interf. Sci.* **166**, 51-60.

Koper G. J. M. and Borkovec M. (1996b) Exact affinity distributions for linear polyampholytes and polyelectrolytes. *J. Chem. Phys.* **104**, 4204-4213.

Koper G. J. M. and Borkovec M. (1996a) Exact affinity distributions for linear polyampholytes and polyelectrolytes. *J. Chem. Phys.* **104**, 4204-4213.

Mathuthu A. S. and Ephraim J. H. (1995) Binding of cadmium to Laurentide fulvic acid. Justification of the functionalities assigned to the predominant acidic moieties in the fulvic acid molecule. *Talanta* **42**, 1803-1810.

Mathuthu A. S., Marinsky J. A., and Ephraim J. H. (1995) Dissociation Properties of Laurentide Fulvic-Acid - Identifying the Predominant Acidic Sites. *Talanta* **42**, 441-447.

Merz P. H. (1980) Determination of Adsorption Energy-Distribution by Regularization and A Characterization of Certain Adsorption-Isotherms. *J. Comp. Chem.* **38**, 64-85.

Milne C. J., Kinniburgh D. G., Dewit J. C. M., van Riemsdijk W. H., and Koopal L. K. (1995) Analysis of proton binding by a peat humic-acid using a simple electrostatic model. *Geochim. Cosmochim. Ac.* **59**, 1101-1112.

Milne C. J., Kinniburgh D. G., van Riemsdijk W. H., and Tipping E. (2003) Generic NICA-Donnan model parameters for metal-ion binding by humic substances. *Environ. Sci. Technol.* **37**, 958-971.

Puy J., Galceran J., Huidobro C., Companys E., Samper N., Garcés J. L., and Mas F. (2008) Conditional Affinity Spectra of Pb^{2+}-Humic Acid Complexation from Data Obtained with AGNES. *Environ. Sci. Technol.* **42**, 9289-9295.

Puy J., Huidobro C., David C., Rey-Castro C., Salvador J., Companys E., Garces J. L., Galceran J., Cecilia J., and Mas F. (2009) Conditional affinity spectra underlying NICA isotherm. *Colloids Surf. A* **347**, 156-166.

Rey-Castro C., Mongin S., Huidobro C., David C., Salvador J., Garces J. L., Galceran J., Mas F., and Puy J. (2009) Effective Affinity Distribution for the Binding of Metal Ions to a Generic Fulvic Acid in Natural Waters. *Environ. Sci. Technol.* **43**, 7184-7191.

Rusch U., Borkovec M., Daicic J., and van Riemsdijk W. H. (1997) Interpretation of competitive adsorption isotherms in terms of affinity distributions. *J. Colloid. Interf. Sci.* **191**, 247-255.

Ruzic I. (1996) Trace metal complexation at heterogeneous binding sites in aquatic systems. *Mar. Chem.* **53**, 1-15.

Sips R. (1948) On the structure of a catalyst surface. *J. Chem. Phys.* **16**, 490-495.

Tipping E. (1998) Humic ion-binding model VI: An improved description of the interactions of protons and metal ions with humic substances. *Aquatic Geochemistry* **4**, 3-48.

Tipping E. (2002) *Cation binding by humic substances*. Cambridge University Press, Cambridge (UK).

Tipping E. and Hurley M. A. (1992) A unifying model of cation binding by humic substances. *Geochim. Cosmochim. Ac.* **56**, 3627-3641.

Tipping E., Rey-Castro C., Bryan S. E., and Hamilton-Taylor J. (2002) Al(III) and Fe(III) binding by humic substances in freshwaters, and implications for trace metal speciation. *Geochim. Cosmochim. Ac.* **66**, 3211-3224.

van Dijk H. (1971) Cation binding of Humic Acids. *Geoderma* **5**, 53-66.

van Riemsdijk W. H., Bolt G. H., Koopal L. K., and Blaakmeer J. (1986) Electrolyte adsorption on heterogeneous surfaces - Adsorption models. *J. Colloid. Interf. Sci.* **109**, 219-228.

Vos C. H. W. and Koopal L. K. (1985) Surface Heterogeneity Analysis by Gas-Adsorption - Improved Calculation of the Adsorption Energy-Distribution Function Using A New Algorithm Named Caesar. *J. Colloid. Interf. Sci.* **105**, 183-196.

Brief

Cd and Pb-Humic Acid binding data from proton titrations at fixed total metal concentrations have been interpreted with the conditional affinity spectrum at total metal (and HA) concentration underlying NICA isotherm.

Tables

Table 1. NICA parameters retrieved by fitting proton titrations of Humic Acid in 0.1M KNO_3 in the absence/presence of Pb/Cd at fixed total concentrations, using glass electrode data only. The uncertainty is expressed as 95% confidence intervals. The parameter values were not constrained in the analysis of uncertainty of the non-linear regression.

NICA Parameters of proton							
$Q_{max,1}$ / mol kg^{-1}	log ($\bar{k}_{H,1}$ /	$n_{H,1}$	p_1	$Q_{max,2}$ / mol kg^{-1}	log ($\bar{k}_{H,2}$ /	$n_{H,2}$	p_2

	M^{-1})				M^{-1})		
4.6 ± 0.5	4.6 ± 0.3	0.48± 0.08	0.64± 0.04	3.0 ± 0.9	11.1 ± 0.7	0.9 ± 0.2 [1]	0.5 ± 0.1

NICA Parameters of Lead			
log ($\bar{k}_{Pb,1}$ / M^{-1})	$n_{Pb,1}$	log ($\bar{k}_{Pb,2}$ / M^{-1})	$n_{Pb,2}$
4.2 ± 0.1	0.40 ± 0.04	10.2 ± 0.7	0.7 ± 0.1

NICA Parameters of Cadmium			
log ($\bar{k}_{Cd,1}$ / M^{-1})	$n_{Cd,1}$	log ($\bar{k}_{Cd,2}$ / M^{-1})	$n_{Cd,2}$
2.3 ± 0.1	0.43 ± 0.05	6.4 ± 0.7	0.7 ± 0.1

Table 2: NICA parameters retrieved by fitting proton titrations of Humic Acid in 0.1M KNO_3 in the absence/presence of Pb/Cd at fixed total concentrations, using both glass electrode and metal ISE data simultaneously. The uncertainty is expressed as 95% confidence intervals. The parameter values were not constrained for the analysis of uncertainty in the non-linear regression. [1] Confidence interval between 0 and 1.

NICA Parameters of proton							
$Q_{max,1}$ / mol kg^{-1}	log ($\bar{k}_{H,1}$ / M^{-1})	$n_{H,1}$	p_1	$Q_{max,2}$ / mol kg^{-1}	log ($\bar{k}_{H,2}$ / M^{-1})	$n_{H,2}$	p_2
4.6 ± 0.5	4.6 ± 0.3	0.6 [1]	0.5 ± 0.4	3.7 ± 0.3	11 ± 2	1 [1]	0.4 [1]

NICA Parameters of Lead			
log ($\bar{k}_{Pb,1}$ / M^{-1})	$n_{Pb,1}$	log ($\bar{k}_{Pb,2}$ / M^{-1})	$n_{Pb,2}$
4.0 ± 0.8	0.4 [1]	11 ± 3	0.7 [1]

NICA Parameters of Cadmium			
log ($\bar{k}_{Cd,1}$ / M^{-1})	$n_{Cd,1}$	log ($\bar{k}_{Cd,2}$ / M^{-1})	$n_{Cd,2}$
2.2 ± 1.6	0.5 [1]	7 ± 5	0.7 [1]

Figures

Figures

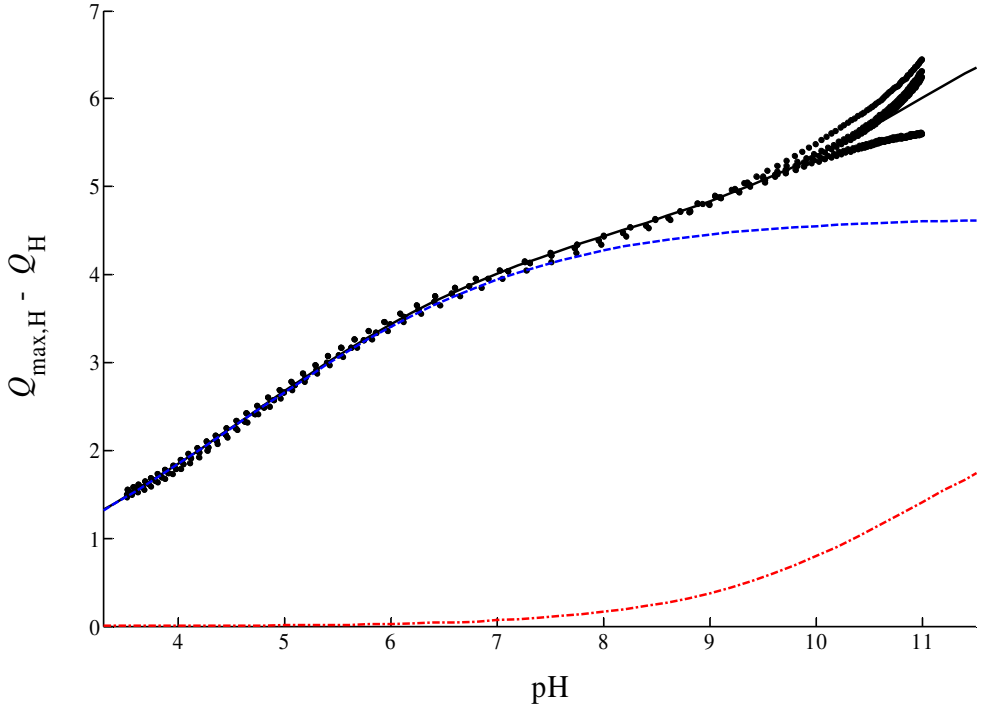

Fig. 1a. Concentration of non-protonated sites $Q_{max,H} - Q_H$ (mol·kg^{-1}) of HA as a function of pH, in absence of added metal. All experiments throughout this work were performed in 0.1M KNO_3 background electrolyte. Symbols: experimental data corresponding to four titration replicates; black solid line: NICA model fit using parameters listed in Table 1; blue dashed line: sites of the "carboxylic" distribution; red dashed-dotted line: sites of the "phenolic" distribution.

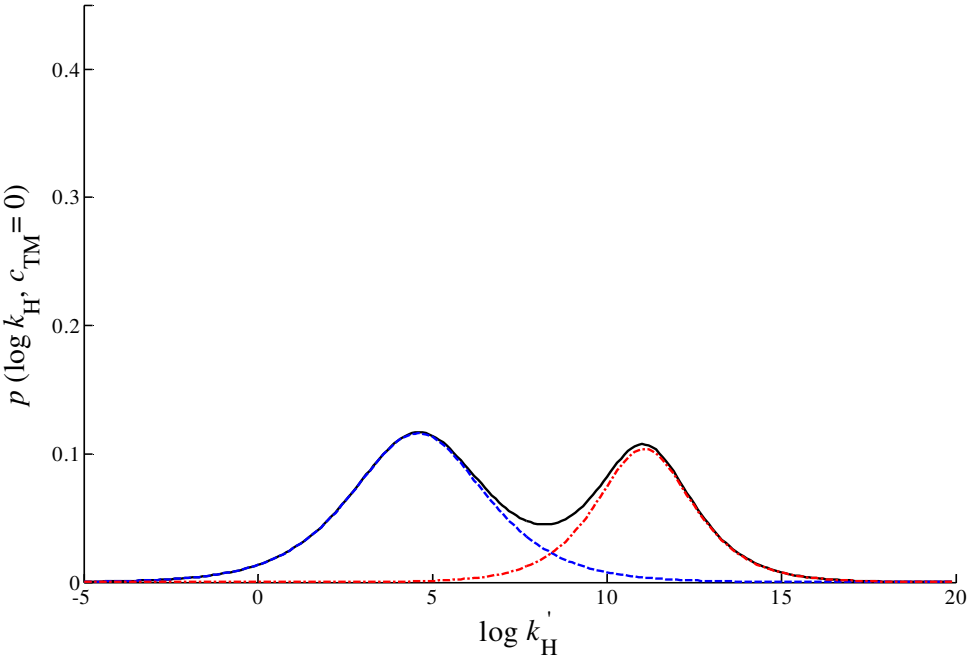

Fig. 1b Affinity spectrum of the HA for protons in absence of metal. In these conditions (binding of H^+ only) NICA model reduces to the Langmuir-Freundlich isotherm and the corresponding affinity spectrum (continuous line) is a bimodal Sips distribution with parameters given in Table 1. Dashed lines stand for the individual modal distributions.

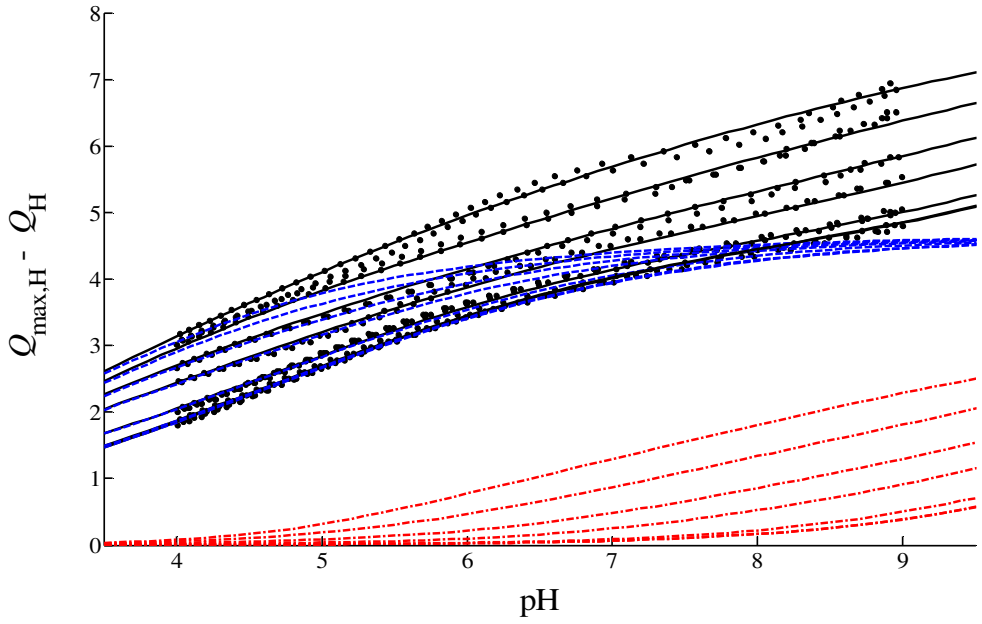

Fig 2. Concentration of non-protonated sites $Q_{max,H} - Q_H$ (mol·kg^{-1}) as a function of pH in the presence of a fixed total lead concentration, $c_{T,Pb}$, of 0; 10^{-5}; 10^{-4}; 3.16×10^{-4}; 5×10^{-4}; 7.5×10^{-4}; and 10^{-3} M (from bottom to top). Symbols and lines as in Fig 1a. Note that the curves corresponding to $c_{T,Pb} = 0$ and 10^{-5} M overlap. The typical repeatability of the experiments is indicated by plotting two titration replicates for each metal concentration.

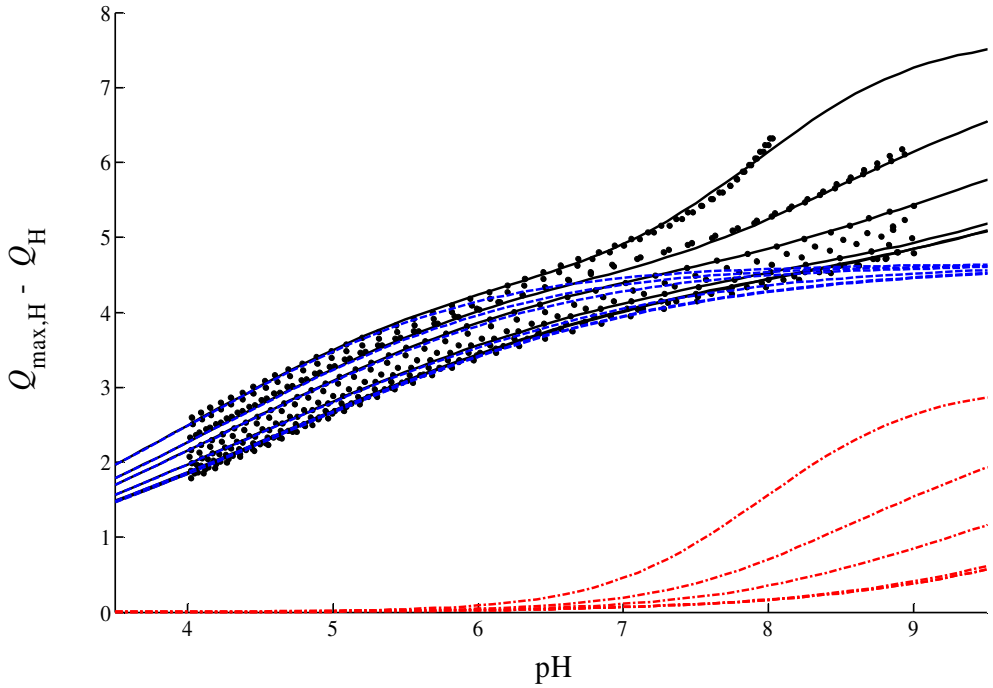

Fig. 3. Concentration of non-protonated sites $Q_{max,H} - Q_H$ (mol·kg^{-1}) as a function of pH in the presence of a fixed total cadmium concentration, $c_{T,Cd}$, of. 0; 10^{-5}; 10^{-4}; 5×10^{-4}; 10^{-3}; and 3×10^{-3} M (from bottom to top). Symbols and lines as in Fig 1a. Note that the curves corresponding to $c_{T,Cd}$ = 0 and 10^{-5} M overlap. The typical repeatability of the experiments is indicated by plotting two titration replicates for each metal concentration.

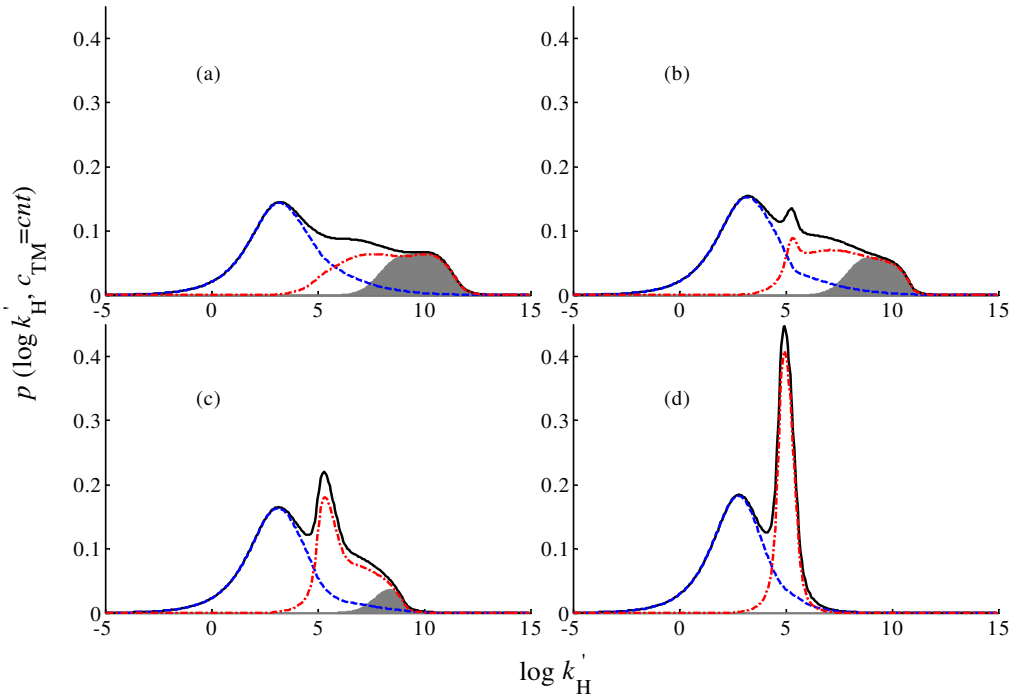

Fig 4. CAScTM of the HA for protons at different fixed total lead concentrations. Black solid line: global spectrum; blue dashed line: "carboxylic" distribution; red dashed-dotted line: "phenolic" distribution; grey shaded area: distribution of sites occupied by protons at pH = 8. $c_{T,Pb} = 7.5\times10^{-4}$ M (a); 10^{-3}M (b); 1.5×10^{-3}M (c); and. 5×10^{-3}M (d)

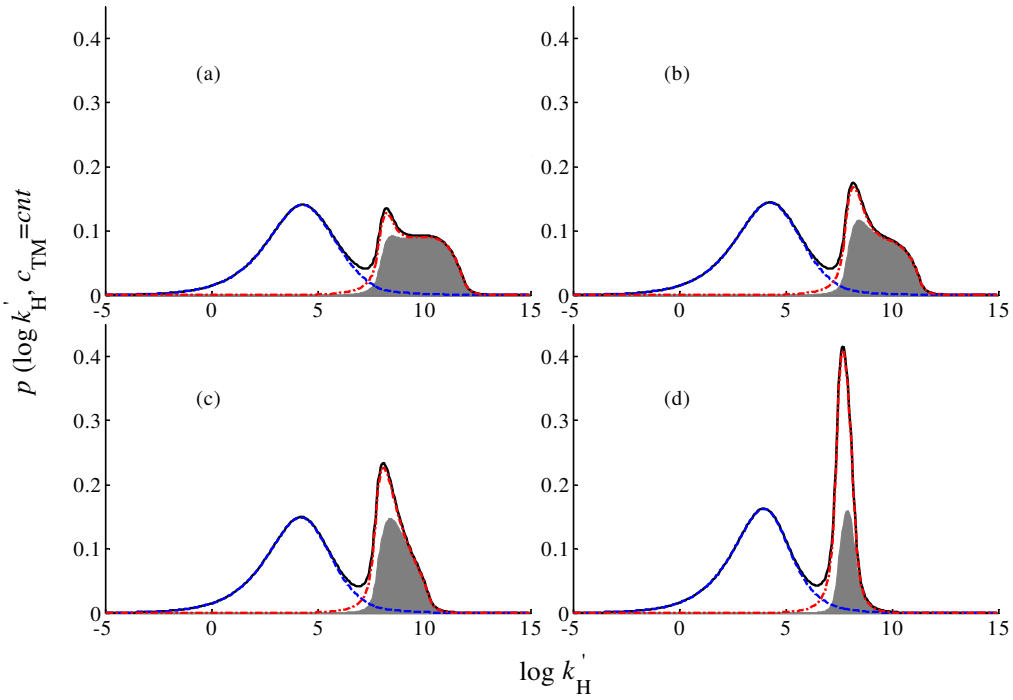

Fig 5. CAScTM of the HA for protons at different fixed total cadmium concentrations. Conventions as in Fig 4. $c_{T,Cd} = 7.5\times10^{-4}$ M (a); 10^{-3}M (b); 1.5×10^{-3}M (c); and, 5×10^{-3}M (d)

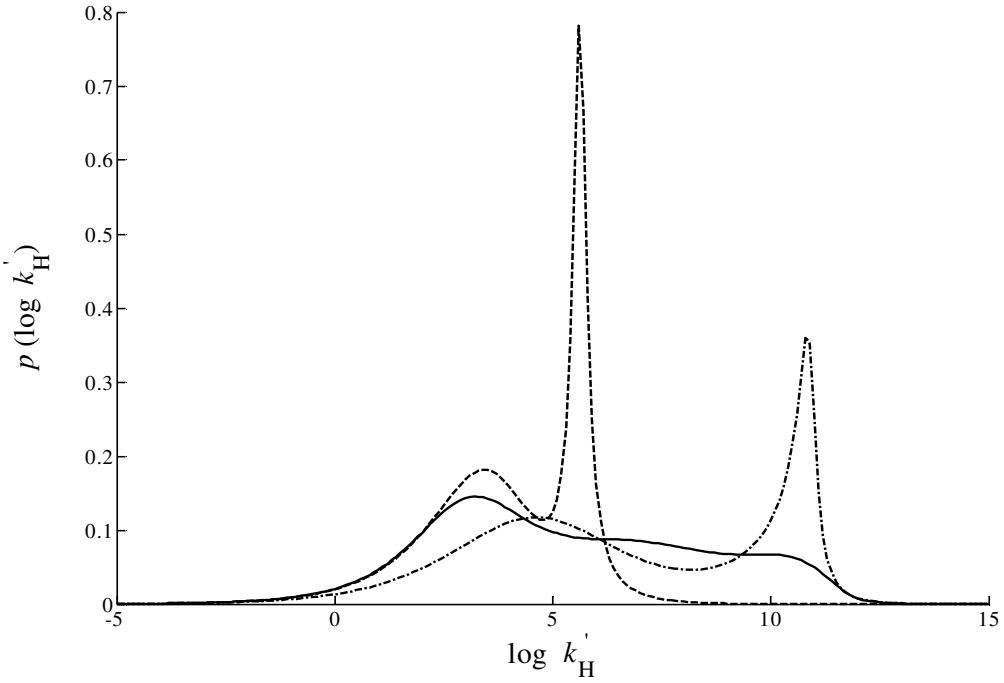

Fig. 6. Solid line: CAScTM of the HA for protons at a fixed total lead concentration of $c_{T,Pb} = 7.5\times10^{-4}$ M; dashed line: CAScM at a constant free lead concentration $c_{Pb} = 5.6\times10^{-4}$M, corresponding to $c_{T,Pb} = 7.5\times10^{-4}$ M and pH=4; dashed-dotted line: CAScM at a constant free lead concentration $c_{Pb} = 10^{-10}$ M, corresponding to $c_{T,Pb} = 7.5\times10^{-4}$ M and pH=10.

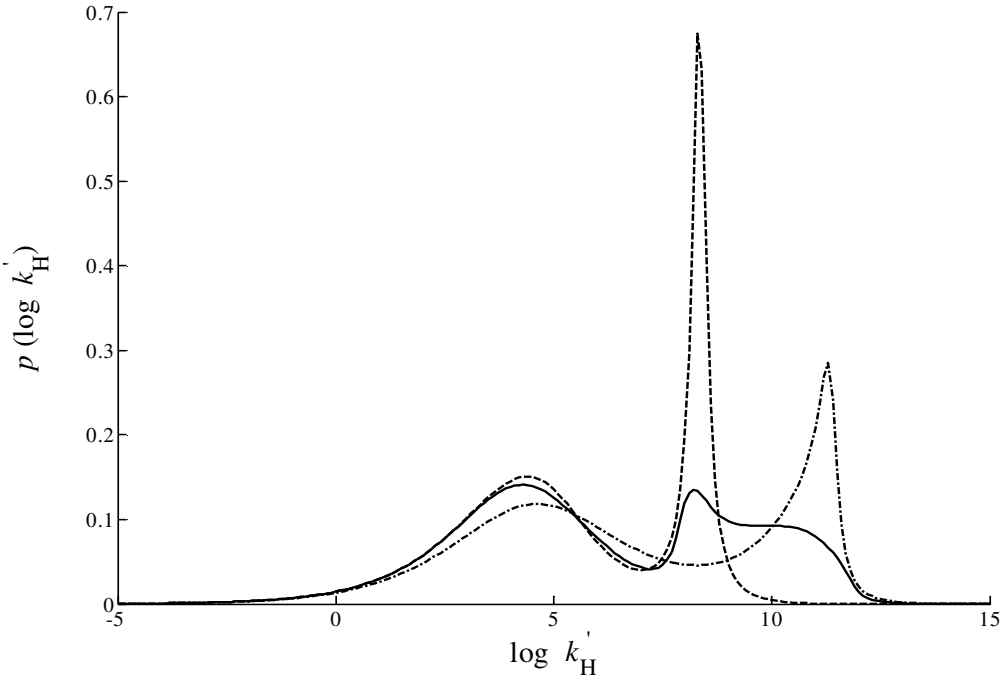

Fig. 7. Solid line: CAScTM of the HA for protons at a fixed total cadmium concentration of $c_{T,Cd}$ = 7.5×10^{-4} M; dashed line: CAScM at a constant free cadmium concentration $c_{Cd} = 7.1\times10^{-4}$M corresponding to $c_{T,Cd} = 7.5\times10^{-4}$ M and pH=4 ; dashed-dotted line: CAScM at a constant free cadmium concentration $c_{Cd} = 1.6\times10^{-7}$ M, corresponding to $c_{T,Cd} = 7.5\times10^{-4}$ M and pH=10.